THE HONG KONG UNIVERSIT OF SCIENCE AND TECHNOLOGY | LIBRARY

HKUST SPD - INSTITUTIONAL REPOSITORY

Title	Carrier Concentration Reduction by Fluorine Doping in P-Type SnO Thin-Film Transistors
Authors	Wang, Sisi; Lu, Lei; Li, Jiapeng; Xia, Zhihe; Kwok, Hoi Sing; Wong, Man
Source	Digest of Technical Papers - SID International Symposium, v. 50, (1), June 2019, article number P-11, p. 1251-1254, Book 3: Active-Matrix Devices Posters
Version	Accepted Version
DOI	10.1002/sdtp.13160
Publisher	John Wiley & Sons, Inc.
Copyright	This is the peer reviewed version of the following article: Wang, S., Lu, L., Li, J., Xia, Z., Kwok, H.S. and Wong, M. (2019), P-11: Carrier Concentration Reduction by Fluorine Doping in P-Type SnO Thin-Film Transistors. SID Symposium Digest of Tech
License	CC-BY-NC 4.0

This version is available at HKUST SPD - Institutional Repository (https://repository.ust.hk/ir)

If it is the author's pre-published version, changes introduced as a result of publishing processes such as copy-editing and formatting may not be reflected in this document. For a definitive version of this work, please refer to the published version.

Carrier concentration reduction by fluorine doping in p-type SnO thin-film transistors

Sisi Wang[1], Lei Lu[1,2], Jiapeng Li[1], Zhihe Xia[1], Hoi Sing Kwok[1,2] and Man Wong[1]

[1]Department of Electronic and Computer Engineering,

[2]The Jockey Club Institute for Advanced Study,

The Hong Kong University of Science and Technology, Clear Water Bay, Kowloon, Hong Kong.

Abstract

Presently reported is the use of plasma fluorination treatment based on tetrafluoromethane to enhance the performance of a p-type SnO thin-film transistor (TFT). The improved performance metrics include a larger on/off current ratio, a smaller subthreshold swing and a reduction of an originally large positive turn-on voltage. The effects of such fluorination treatment were also investigated using a host of thin-film characterization techniques and their origin most plausibly attributed to both the significant reduction of the carrier concentration from $\sim 2 \times 10^{19}$ ***cm***$^{-3}$ ***to*** $\sim 4.3 \times 10^{16}$ ***cm***$^{-3}$ ***and the passivation of the defects. It is demonstrated that fluorination is an effective technique for making higher performance p-type metal-oxide TFTs.***

Author Keywords

p-type, tin oxide, thin-film transistor, fluorine.

1. Introduction

Thin-film transistors (TFTs) based on metal-oxide semiconductors have attracted much attention, especially in the flat-panel display industry [1], due to their good uniformity, high optical transparency, moderately high carrier mobility and relatively low-temperature processing. Compared with the more mature n-type metal-oxide TFTs, such as those based on zinc oxide and its variants, there is a limited choice of p-type metal-oxide TFTs exhibiting sufficient performance and worthy of integration with their n-type counterparts to realize potential low-power complementary circuits [2-4].

With a valence band composed of hybridized tin (Sn) 5*s* and oxygen (O) 2*p* orbitals, tetragonal tin (II) oxide (SnO) has been popularly investigated among several metal-oxide semiconductors for the realization of p-type TFTs. There are two critical but unresolved issues that hinder the practical applications of p-type SnO TFT. These are the small on/off current ratio and the poor subthreshold swing (*SS*), respectively attributed to the relatively high background hole concentration (typically around 10^{18} cm^{-3} [2, 5]) and the high density of the interface or bulk sub-gap states [2, 6].

The approach taken in the present investigation is to reduce the high background hole concentration in the channel of a SnO TFT through the incorporation of compensating donors. When a 25-nm thick SnO thin film was treated in a tetrafluoromethane (CF_4) plasma, the background hole concentration estimated using Hall Effect measurement was found to decrease by more than two orders of magnitude. This is presently attributed to the introduction of donors formed by the substitution of O^{2-} by F^-. Benefited from the reduced background carrier concentration, the on/off current ratio increased from 285 to 987, *SS* decreased and the turn-on voltage (V_{on}) negatively shifted from 10.1 V to 0.9 V. The last item is important since it makes the TFT much less of depletion-mode device.

2. Experimental

The bottom-gate SnO TFTs were fabricated on a heavily doped n-type silicon substrate with a 100-nm thick thermal oxide as the gate dielectric. The substrate doubled as the gate electrode of a TFT. A 25-nm thick SnO active layer was next deposited by DC magnetron sputtering at room-temperature using a pure Sn target. Active islands were subsequently patterned and etched using a chlorine-based chemistry. A select group of TFTs were treated in a CF_4 plasma at 100°C for different durations. Patterned using a lift-off process, a 100-nm thick Ni was then evaporated as the source/drain (S/D) electrodes. The SnO active layer was crystallized at 300°C in an oxygen atmosphere for 10 minutes. Finally, an aluminum oxide (AlO) passivation layer was deposited using pulsed-DC sputtering of a pure Al target. A schematic cross-section of the resulting bottom-gate SnO TFT is shown in Figure 1. The characteristics of the TFTs were measured using an Agilent 4156C Semiconductor Parameter Analyzer.

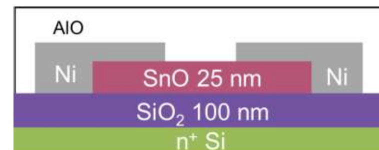

Figure 1. The cross-section of a bottom-gate SnO TFT.

100-nm thick SnO thin films were also separately prepared using the same fabrication process. These thicker films were characterized using x-ray diffraction (XRD), x-ray photoelectron spectroscopy (XPS) and secondary ion-mass spectrometry (SIMS) to determine, respectively, the quality of the crystallization, the elemental composition and the corresponding chemical states, and spatial distribution of the constituent elements. Room-temperature Hall Effect measurement was employed to measure the resistivity of the film, together with the type and population of the charge carriers.

3. Results and Discussion

The as-deposited SnO and the fluorinated SnO (SnO:F) were amorphous. The XRD spectra (Fig. 2) taken after a heat-treatment at 300°C in an oxygen atmosphere for 10 minutes confirmed the crystallization of both SnO and SnO:F samples, with a preferential

orientation along the [101] directions. For the SnO:F samples, the main peak is broadened without altering the relative abundance of the orientations. Using the Scherrer equation [7], the average grain size of the samples is estimated, with the 60s-fluorinated SnO:F exhibiting an average grain size of 15.4 nm, a slight reduction compared to the average grain size of 16.54 nm of the untreated SnO samples.

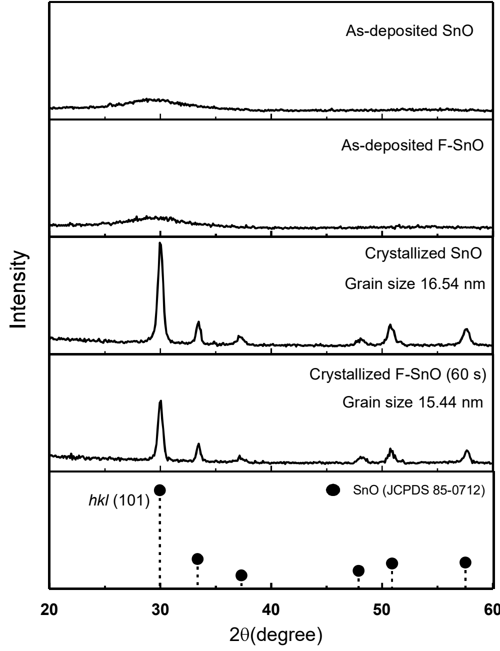

Figure 2. The XRD spectra of the SnO:F and the untreated SnO thin films.

The Hall-Effect electrical characterization results are shown in Figure 3. A high hole concentration (n_h) of $\mathbf{2 \times 10^{19}}$ cm^{-3} is obtained in the untreated SnO film, with a resistivity (ρ) of 0.5 $\Omega \cdot$cm and a Hall mobility (μ_{Hall}) of 1 cm^2/Vs. These are comparable to those reported in the literature [8-9].

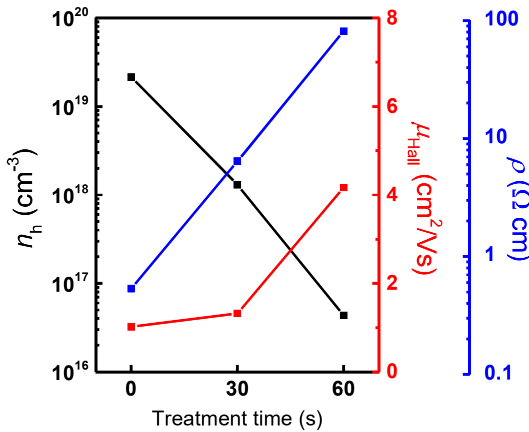

Figure 3. The average hole concentration (n_h), resistivity (ρ) and hall mobility (μ_{Hall}) of the SnO film, extracted from room temperature Hall-effect measurements. The SnO film was fluorinated for different durations.

When the fluorination treatment time was increased from 0 s to 60 s, n_h significantly decreased to $\mathbf{4.3 \times 10^{16}}$ cm^{-3}, ρ increased to 81 $\Omega \cdot$cm and μ_{Hall} slightly increased to 4.1 cm^2/Vs. The reduced n_h and increased ρ demonstrate the effective doping effect of the fluorination treatment. The higher μ_{Hall} may have resulted from the smaller grain size of the SnO:F thin film in the localized-trap-states model [10]. The smaller grain size can reduce the free carrier concentration inside the polycrystalline thin-film by the carrier trapping at the localized trap states at the grain boundaries. When the number of trap states per unit volume is larger than the free carrier concentration, because the trap states are not completely filled, the potential barrier height at the grain boundaries are relatively low. The reduced grain boundary scattering increases the carrier mobility inside the polycrystalline thin-film. When the treatment time was increased to 90 s, ρ became too large and exceeded the measurement range of the equipment.

The XPS was used to examine the nature and the chemical states of the constituents of the samples. Before the measurement, an argon plasma was applied to remove surface contamination. Shown in Figure 4 is the dependence on fluorination time of the $Sn3d_{5/2}$ spectra of the SnO thin films. Peaks around 486.6 eV were consistently observed, corresponding to the presence of Sn^{2+} [11].

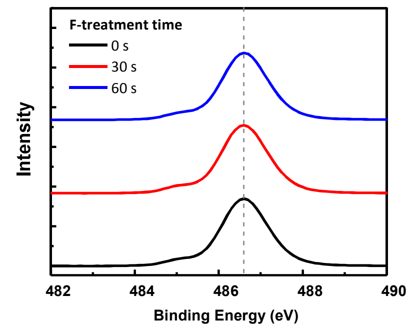

Figure 4. Sn $3d_{5/2}$ XPS spectra of SnO thin films subjected for different fluorination treatment times.

By observing of Sn $3d_{5/2}$ XPS spectra, besides Sn^{2+}, other chemical states of the Sn (Sn^0, and Sn^{4+}) in SnO:F is subtle in this plasma treatment, suggesting that the carrier reduction does not originate from the mixture of the Sn oxides with different chemical states. The atomic concentration before and after the crystallization process in oxygen is summarized in Table I.

Table I. The atomic concentration of the SnO:F thin film before and after the 300°C crystallization in oxygen.

Element	Sn%	O%	F%	Sn:O:F	O:F
	As-deposited				
0s	55.18	43.68	0.36*	1:0.79:0.080*	*
30s	56.10	41.22	1.82	1:0.73:0.044	22.65
60s	56.73	40.01	2.45	1:0.71:0.060	16.33
	Crystallized				
0s	54.77	44.10	0.27*	1:0.81:0.006*	*
30s	54.52	43.72	0.95	1:0.80:0.022	46.02
60s	54.62	43.1	1.45	1:0.79:0.034	29.72

Because the SnO is metastable, the stoichiometry control during the sputtering process is a challenge. The deposited SnO thin films were in a Sn-riched status, which was designed to execute the post-deposition stoichiometry adjustment during the crystallization process in an oxygen atmosphere. As observed in the Table I, before the annealing process for crystallization, the fluorination process reduced the oxygen concentration in SnO:F. When the fluorination duration increased from 0 s to 60 s, the atomic ratio of Sn:O increased from 1:0.79 to 1:0.71, which demonstrate the cooperation of F and implied the substitutison of O by F. After the annealing process in oxygen, the differences between the SnO and SnO:F thin films decreased. The atomic ratio of Sn:O was adjusted to 1:0.81 for SnO, and 1:0.80(1:0.79) for SnO:F 30 s (60 s). On the one hand, a more desirable stoichiometry of the SnO was achieved. On the other hand, the possible disadvantage of the stoichiometry change of SnO:F was lessened. In both unannealed and annealed samples, the atomic ratio of O:F decreases with the increase of the fluorine treatment time, which may have resulted from the substitution of O^{2-} by F^{-}. The F concentration detected in the un-treated sample was due to possible contamination during the measurement, marked with an asterisk (*). The distribution of F in SnO:F before and after the crystallization process was characterized using SIMS and shown in Figure 5. This redistribution of F atoms during the annealing process caused the F concentration decreased after the annealing process listed Table I. Because the examined depth is near the treated front surface.

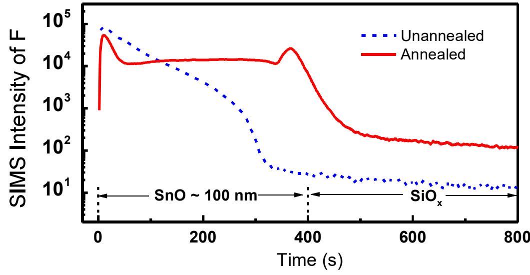

Figure 5. The SIMS depth profiles of F in SnO: before and after the thermal crystallization process.

Shown in Figure 6 and Table II are the respective normalized drain current ($I_d/(W/L)$) versus gate voltage (V_g) transfer characteristics of the SnO TFTs, and the transistor parameters extracted from the Figure 6.

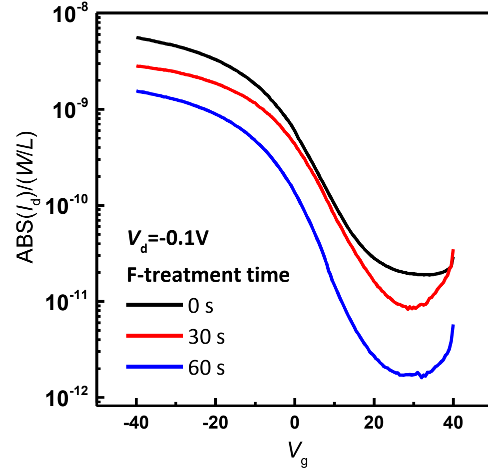

Figure 6. The transfer characteristics of SnO and F-SnO TFTs with the fluorine treatment time from 0s to 60s.

The channel width W is 100 µm. The V_{on} is defined as the V_g needed to induce an I_d of 100 pA in the subthreshold region. As the fluorine plasma treatment time increased from 0 s to 60 s, the off-current decreased from 18 pA to 1.6 pA at a drain voltage of -0.1 V. The on/off ratio increased from 285 to 987, whereas the SS decreased from 12.2 to 7.1 V/dec. The improved on/off ratio and SS can be attributed to the higher channel resistance and potential passivation of traps. The large negative shift of V_{on} from 10.1 V to 0.9 V is attributed to the reduction of the total carrier concentration in the SnO:F. When the treatment time increased to 90 s, the on current was also drastically degraded (not shown here), which may result from either the plasma damage or poor source/drain contacts.

Table II. The extracted parameters of the SnO and SnO:F TFTs.

Time	SS (V/dec)	on/off ratio	V_{on} (V) @100 pA
0s	12.2	285	10.1
30s	10.5	337	8.6
60s	7.1	987	0.9

5. Conclusion

When treated with a CF_4 plasma, the background hole concentration in the subsequently crystallized SnO:F thin film was reduced from $\sim 2 \times 10^{19}$ cm^{-3} to $\sim 4.3 \times 10^{16}$ cm^{-3}, and the corresponding resistivity increased from 0.5 to 81 Ω·cm. This reduction in the background concentration may have resulted from compensation doping by donors generated by the replacement of O^{2-} by F^{-}. Benefiting from the reduction of the background carrier concentration, the corresponding p-type SnO:F TFTs exhibit better performance, including larger on/off current ratio, smaller SS and the reduction of V_{on} from 10.1 V to 0.9 V. The characteristics of SnO:F TFTs, if further improved, could eventually enable the realization of low-power circuits consisting of complementary n- and p-channel metal-oxide TFTs.

6. Acknowledgment

This work was supported by Grant No. GHP/022/12SZ-2 from the Innovation and Technology Fund and No. ITC-PSKL12EG02 from the Partner State Key Laboratory on Advanced Displays and Optoelectronics Technologies. The TFTs were fabricated at the Nanosystem Fabrication Facility of HKUST.

7. References

[1] Fortunato, Elvira, Pedro Barquinha, and R. Martins. "Oxide semiconductor thin- film transistors: a review of recent advances." Advanced materials 24.22 (2012): 2945-2986.

[2] Ogo, Yoichi, Hidenori Hiramatsu, Kenji Nomura, Hiroshi Yanagi, Toshio Kamiya, Masahiro Hirano, and Hideo Hosono. "p-channel thin-film transistor using p-type oxide semiconductor, SnO." Applied Physics Letters 93, no. 3 (2008): 032113.

[3] Fortunato, Elvira, Raquel Barros, Pedro Barquinha, Vitor Figueiredo, Sang-Hee Ko Park, Chi-Sun Hwang, and Rodrigo Martins. "Transparent p-type SnO x thin film transistors produced by reactive rf magnetron sputtering followed by low temperature annealing." Applied Physics Letters 97, no. 5 (2010): 052105.s

[4] Ogo, Yoichi, Hidenori Hiramatsu, Kenji Nomura, Hiroshi Yanagi, Toshio Kamiya, Mutsumi Kimura, Masahiro Hirano, and Hideo Hosono. "Tin monoxide as an s-orbital-based p-type oxide semiconductor: Electronic structures and TFT application." physica status solidi (a) 206, no. 9 (2009): 2187-2191.

[5] Nomura, Kenji, Toshio Kamiya, and Hideo Hosono. "Ambipolar oxide thin-film transistor." Advanced Materials 23, no. 30 (2011): 3431-3434.

[6] Wang, Zhenwei, Pradipta K. Nayak, Jesus A. Caraveo-Frescas, and Husam N. Alshareef. "Recent developments in p-Type oxide semiconductor materials and devices." Advanced Materials 28, no. 20 (2016): 3831-3892.

[7] Cullity, Bernard Dennis. "Elements of X-ray diffraction, Addison." Wesley Mass (1978).

[8] Lee, Seung Jun, Younjin Jang, Han Joon Kim, Eun Suk Hwang, Seok Min Jeon, Jun Shik Kim, Taehwan Moon et al. "Composition, Microstructure, and Electrical Performance of Sputtered SnO Thin Films for p-Type Oxide Semiconductor." ACS applied materials & interfaces 10, no. 4 (2018): 3810-3821.

[9] Guzmán-Caballero, D. E., M. A. Quevedo-López, W. De la Cruz, and R. Ramírez-Bon. "Fully patterned p-channel SnO TFTs using transparent Al2O3 gate insulator and ITO as source and drain contacts." Semiconductor Science and Technology 33, no. 3 (2018): 035010.

[10] Higashi, Seiichiro, Kentaro Ozaki, Keiji Sakamoto, Yoshiaki Kano, and Toshiyuki Sameshima. "Electrical properties of excimer-laser-crystallized lightly doped polycrystalline silicon films." Japanese journal of applied physics 38, no. 8A (1999): L857.

[11] Lin, Albert WC, Neal R. Armstrong, and Theodore Kuwana. "X-ray photoelectron/Auger electron spectroscopic studies of tin and indium metal foils and oxides." Analytical Chemistry 49, no. 8 (1977): 1228-1235.s